Indian Journal of Chemical Technology
Vol. 28, May 2021, pp. 319-327

Adsorptive column studies for removal of acid orange 7 dye using bagasse fly ash

Sunil Deokar[1], Himanshu Patel[2], Priyanka Thakare[3], Sanjay Bhagat[4], Vidyadhar V Gedam[5] & Pranav Pathak*[,6]

[1]Anuradha Engineering College, Chikhli, India
[2]Pacific School of Engineering, Surat, India
[3]SSBT's College of Engineering & Technology, Jalgaon, India
[4]PVPIT, Budhgaon, Sangli, India
[5]National Institute of Industrial Engineering (NITIE), Mumbai.Maharashtra, India
[6]MIT School of Bioengineering Sciences & Research, Pune, India

E-mail: sunildeokar2008@gmail.com

Received 23 April 2020; accepted 26 March 2021

Increasing industrialization creates a large scale of pollution and affects the availability of usable water. Dyes in wastewater are a visible pollutant, difficult to treat, and are toxic in nature. Amongst all the physicochemical methods, adsorption is the extensively applied process for the aqueous removal of dye. In the present study; the Bagasse Fly Ash (BFA) is used as an adsorbent for aqueous removal of Acid Orange dye in packed bed adsorption technique. The packed bed studies for different bed heights, influent concentration and flow rate are performed. The efficacy of packed columns is investigated using different models namely Bed depth service time, Thomas, Wolborsaka, Yoon-Nelson, and Bohart-Adams Models. The maximum adsorption capacity of BFA for 50% saturation of column is calculated to be 38 (mg/g) which shows BFA as a good adsorbent for dye removal.

Keywords: Acid orange 7 dye, Bagasse fly ash, Packed bed, Packed bed models

In the last decade, industrial pollution and global warming show an adverse effect on water resources which results in scarcity of good quality water. The treatment of wastewater is essential for an environment devoid of pollution as well as to meet the water need of the community[1]. Major pollutants from food processing, cosmetics, paper, dye manufacturing, textile, and printing are colours left by dyes in wastewater[2,3]. These dyes include many different compounds whose environmental behaviour is unknown. Most of the dyes used are toxic and carcinogenic in nature. The presence of dyes in the water body is opposed to environmental conditions like light, the consequence of *p*H, and microbial attack. Therefore, the existence of dyes in the water body is unwanted and needs to be removed before wastewater comes in contact with water bodies. A number of processes such as filtration, sedimentation, chemical oxidation, biological treatment, adsorption are used for water treatment[4-6]. Among the aforesaid methods, the adsorption process is the cheapest one due to its low cost, flexibility, and ease of operation. Additionally, adsorption does not create a large quantity of waste sludge[1,5,7]. Recently it has been used as an effective and economic treatment for the adsorptive removal of dye from water. Adsorption is carried out with activated carbon in a conventional adsorption system which is expensive and needs regeneration[8]. Therefore it results in the search for inexpensive adsorbent material for adsorptive removal of colouring dye from industrial effluents. One potential approach is the usage of Bagasse Fly Ash (BFA) as an inexpensive adsorbent. According to the Food and Agricultural Organization of the United Nations (FAO 2014); out of 12 million tons of global generation, 2 million tons of BFA is only generated in India[9]. Therefore these data of ash generation in large quantity as waste in sugar-power industries indicates that there is a need to use BFA again to overcome the disposal problem. The physico-chemical characterization of BFA reported in previous studies indicated the presence of carbon, silica, and trace quantities of metal oxides[10]. Previous studies showed the successful utilization of BFA in the removal of pesticides, heavy metals, and phenolic compounds[11,12]. BFA has various industrial applications. It is mainly used for the preparation of briquette, cement additives, and cement substitute for construction. It is also used for extraction of mesoporous silica, in the preparations of secondary abrasive in composite, immobilization media in the

bioreactor, water polymer and electrode for comparative deionization, insulating powder, production of refractory bricks, and sand Crete block production. In addition to this, BFA has wide applications in the wastewater treatment as an adsorbent for the adsorption of dyes, organic and inorganic compounds[13,14].

The widely used AO7 dye is a moderately toxic azo dye and its toxicity ranges between high toxic metals or phenolic compounds and other organic compounds such as formalin. The azo group in active azo dye creates harmful effects[15]. As a result, it is essential to eliminate AO7 dye from water. Previously reported studies used algae[16,17], microorganisms[18], biodegradation[19], photo-Fenton process[20], and oxidative radiolysis[21] for removal of AO7 dye from water. In these studies, removal of AO7 is carried out in batch operation only to evaluate the potential of adsorbent and to learn the kinetics of adsorption. However adsorptive removal in a packed bed is economically important since the constant contact between adsorbate and adsorbent permits the proficient usage of the adsorbent and therefore increasing the treatment of the effluent. Furthermore, the continuous removal permits the simultaneous regeneration of the adsorbent.

Therefore in this study, we performed the removal of AO7 dye using BFA in a packed bed and investigated the influence of bed height (adsorbent dosage), influent concentration, and flow rate at constant *p*H. The different packed bed parameters such as breakthrough and saturation times, the volume of solution treated, bed capacity, and length of mass transfer zoneis determined for different conditions. The analysis of breakthrough curves is done using BDST, Thomas, Yoon–Nelson, Wolborsaka, and Bohart- Adams Models.

Experimental Section

Materials

Adsorbent

BFA was supplied by M/s Wainganga Sugar and Power Ltd. Bhandara (India). Bagasse was burned as boiler fuel for in the above industry. The ash, volatile matter, and fixed carbon in BFA were determined by proximate analysis method using IS: 1350 (Part 1)[22]. The surface properties were determined using a surface area analyzer (Micromeritics ASAP 2010 model). The presence of metal oxides in BFA was quantified using an X-ray fluorescence analyzer (PW 2403; PANalytical). The percentage of carbon, hydrogen, nitrogen, and sulfur was detected on an elemental analyzer (Vario MACRO Cube; Elementar, Hanau, Germany). The occurrence of functional groups on the BFA surface was examined by FTIR analysis using Shimadzu IR Affinity-1 model. The morphology of BFA was examined using a scanning electron micrograph (SEM, Leo 1430 VP, Oxford Instruments, UK).

Adsorbate

Acid Orange (AO7) dye was purchased from Sigma Aldrich Bangalore, India. The molecular formula and molar mass of AO7 is $C_{16}H_{11}N_2NaO_4S$ and 350.32 g/moL respectively. Initially, the stock solution having a concentration of 1000 mg/L was made by adding an appropriate quantity of AO7 dye in deionized water. For further experiments, the stock solution was diluted using deionized water. The dilute HCl and NaOH were used to adjust the required *p*H of the solution. The analytical grade reagents were used in experiments. The concentration of AO7 dye was quantified at 482 nm (λ_{max}) using the UV-1800 instrument (Shimadzu, Japan).

Method

Packed bed adsorption

One (cm) internal diameter and 25 (cm) heightened glass columnhaving an outlet at different heights at the top was constructed for packed bed adsorption of AO7 dye. A weighed quantity of BFA as per required bed height was filled forcibly between two supporting layers of glass wool. The reason for utilizing the layers of glass wool was to prevent the flow of the BFA particles together with the effluent of AO7 dye. Before starting the actual experimental runs, the deionized water was passed throughout the bed in a downward direction using gravity to remove trapped air. Later the column was kept in operative for 12 hr in order to keep it in wetted form. From the outlet at the top of the column, the samples were collected intermittently at a constant rate of influent and the concentration of effluent C_t (mg/L) of AO7 dye was measured. Each experiment was carried out ata constant temperature (30±2°C) and solution *p*H ~7.0 (±0.2). The column experiments were carried out as per the conditions shown in Table 1. The plot of (C_t/C_0)versus time (t) called a breakthrough (BT) curve was drawn for every experiment. The breakthrough point (t_b) and exhaustion point (t_e) were

considered at C_t/C_0 = 10% and C_t/C_0 95% respectively.

Determination of packed bed parameters

The breakthrough characteristics and shape of BT curves are essential for the determination of the efficiency of the column. Breakthrough parameters such as breakthrough time (t_b), exhaustion/saturation time (t_e), volumes of solution (V_b,V_e) treated att$_b$ and t_e respectively are important for column design in packed bed adsorption. Further, the time required for the movement of the Mass Transfer Zone(t_δ) also plays important role in the design of the column. The movement of MTZ is defined by equation (1) as[23]:

$$t_\delta = \frac{Ve - Vb}{Q} \quad \ldots(1)$$

Column adsorption capacity at 50% breakthrough (mg/g) is calculated using equation (2) [24].

Table 1 — Experimental conditions for packed bed adsorption of AO7 dye using BFA

Expt. no	Bed height (Z, cm)	Influent concentration (Co, mg/L)	Flow rate (Q, mL/min.)
1	1.1	200	2
2	3.2	200	2
3	5.5	200	2
4	3.2	100	2
5	3.2	200	2
6	3.2	300	2
7	3.2	200	2
8	3.2	200	4
9	3.2	200	6

$$q_{0.5} = \frac{t_{0.5}\, Q\, Co}{m} \quad \ldots(2)$$

where $t_{0.5}$ (min), Q (mL/min), and m (g) are breakthrough time, flow rate, and mass of adsorbent respectively. The mass transfer zone (MTZ) is the section of the adsorbent bed where the solute is most effectively and rapidly adsorbed. Various parameters related to MTZ are determined using the following formulae. The height of MTZ (H_{MTZ}) can be calculated from the following expression (3) [23]

$$H_{MTZ} = Z\frac{t_e - t_b}{t_e} \quad \ldots(3)$$

The moving rate (U_z) of MTZ can be calculated from the formula given by equation (4).[23]

$$U_Z = \frac{H_{MTZ}}{t_\delta} \quad \ldots(4)$$

Packed bed modeling

The performance of the present column study is examined using different models mainly Thomas, BDST, Bohart-Adams, Yoon-Nelson, and Wolborska models[25-28]. The linear forms of these models are illustrated in Table 2; the rate constants and adsorption capacities are investigated using the equation of the plots of the models.

Table 2 — Packed bed models for adsorption of AO7 using BFA

Packed bed adsorption model	Linear Equation	Plot	Parameter ofmodel	
			Rate Constant	Adsorption capacity
Thomas Model	$\ln\left[\left(\frac{C_o}{C_t}\right)-1\right] = \frac{K_{TH}q_o m}{Q} - K_{TH}C_o t$	$\ln[(C_o/C_t)-1]$ vs. t	k_{TH}	q_0
Bed Depth Service Time Model	$t = \frac{N_0}{C_0 F}Z - \frac{1}{K_{BDST}C_0}\ln\left(\frac{C_o}{C_t}-1\right)$	Z vs. t	k_{BDST}	N_o
Bohart-Adams Model	$\ln\frac{C_t}{C_o} = K_{AB}C_o t - K_{AB}N_o\frac{Z}{F}$	$\ln[(C_t/C_o)]$ vs. t	k_{AB}	N_o
Yoon-Nelson Model	$\ln\left(\frac{C_t}{C_o - C_t}\right) = K_{YN}t - tK_{YN}$	$In\left(\frac{C_t}{C_o - C_t}\right)$ vs. t	k_{YN}	q_{0YN}
	$q_{OYN} = \frac{q_{(total)}}{m} = \frac{C_o Q_t}{1000m}\frac{\frac{1}{2}C_o[(Q/1000)\times 2]}{m}$			
Wolborska Model	$\ln\left(\frac{C_t}{C_o}\right) = \frac{\beta C_o t}{N_o} - \frac{\beta Z}{F}$	$\ln(C_t/C_0)$ vs. t	β	N_o

Where, C_o – Influent concentration (mg/L), C_t – Effluent at time t (mg/L), t – time (min), m – Mass of adsorbent (g), Z – Bed height (cm), F - Superficial velocity (m/min), τ - Time required for 50 % breakthrough (min), Q – Flow rate (mL/min)

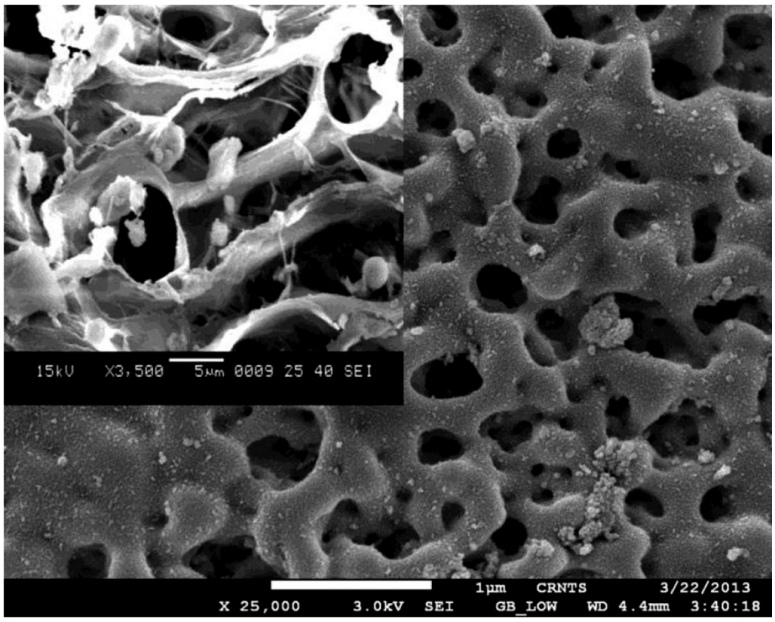

Fig. 1 — Scanning electron micrograph (SEM) of BFA

Results and Discussion

Characteristics of BFA

The proximate analysis of BFA disclosed 6.34% moisture, 42.38% volatile matter, 39.26% ash, andthe remaining 12.02% fixed carbon. The percentage of carbon was found to be 47.37%, which was identified by CHNS analysis. The percentage of silica calculated by XRF analysis was 36.14 together with the minute quantities of metal oxides such as Al_2O_3, K_2O, Fe_2O_3, and CaO. These metal oxides play a vital role in the adsorption process by developing charges on the surface of BFA relying on the *p*H of the solution. Adsorption-desorption isotherm obtained by nitrogen physisorption is given in Fig. S1. According to the classification of isotherms, suggested by Brunauer, Emmett, and Teller[29]; Fig. S1 (Supplementary Information) indicates a behaviour corresponding to type IV isotherm, which is indicative of the mesoporous nature of BFA. A hysteresis loop clearly represented in Fig. S1 (Supplementary Information) could be associated with the capillary condensation of the adsorption/desorption in mesopores. The nitrogen adsorption-desorption method also provides the basis to observe the behaviour of pore size distribution in the adsorbent (Fig. S2 (Supplementary Information)). According to the classification of IUPAC, BFA is mainly mesoporous adsorbent (2 to 50 nm).

The external surface area and the BET surface area of BFA were measured to be 38 m^2/g and 52 m^2/g respectively. The pore diameter and pore volume of BFA were 132 Å and 4.96 × $10^{-2} m^3/g$ respectively. The scanning electron micrograph of BFA given in Fig. 1 shows the porous structure where the elongated, circular, and irregular-shaped pores can be seen. The walls of several circular pores are broken that result in the formation of irregularly shaped pores. In addition, some of the pores look internally connected.

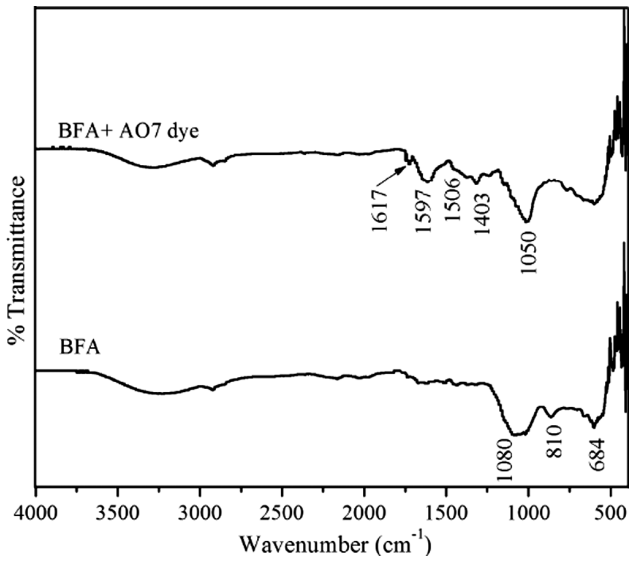

Fig. 2 — FTIR of BFA before and after adsorption of AO7 dye

To confirm the adsorptive removal of AO7 dye on the BFA, the FTIR analysis of BFA is performed before and after adsorption as shown in Fig. 2. The FTIR spectrum of BFA shows the bands at 1080 cm^{-1},

810 $cm^{-1,}$ and 684 cm^{-1} which are allotted to the asymmetric stretching of Si-O-Si, amorphous silica, and stretching vibration of Si-O bond respectively[10]. The BFA spectrum after adsorption of AO7 dye shows the appearance of new peaks in the band of 2000-1000 cm^{-1}owing to the presence of functional groups in AO7 dye. The intense peak at 1597 $cm^{-1}$is characteristic of phenyl group ring vibrations and the small peak at 1506 cm^{-1} is ascribed to the bond of the azo group of AO7 dye[30]. The strong peak at 1050 cm^{-1} is because of the coupling between the benzene and $\upsilon(SO_3)$ whereas the weak peak at 1617 cm^{-1} is a result of the combined effect of the phenyl ring and C=N groupvibrations[30].

Breakthrough curves

The adsorption of AO7 dye molecules in a packed bed relies on the dosage of adsorbent packed in the column. Fig. 3 represents the BT curves for variable bed height (adsorbent dosage) for adsorption of AO7 onto BFA at the fixed concentration (200 mg/L) and flow rate (2 mL/min). The BT curves show that a column having a lower bed height of 1.1 (cm) is exhausted earlier than having a higher bed height (3.2 cm and 5.2 cm). Table 3 shows the breakthrough and exhaust times (t_b and t_e); as well as the volume of solution treated at breakthrough and saturation (V_b and V_e) which are increased with increasing the bed depth. This is because of the greater availability of adsorbent dosage. The adsorption capacity at 50% saturation of column is however decreased with increment in bed height. This is on account of the increase in the length of MTZ with increasing bed height[9].

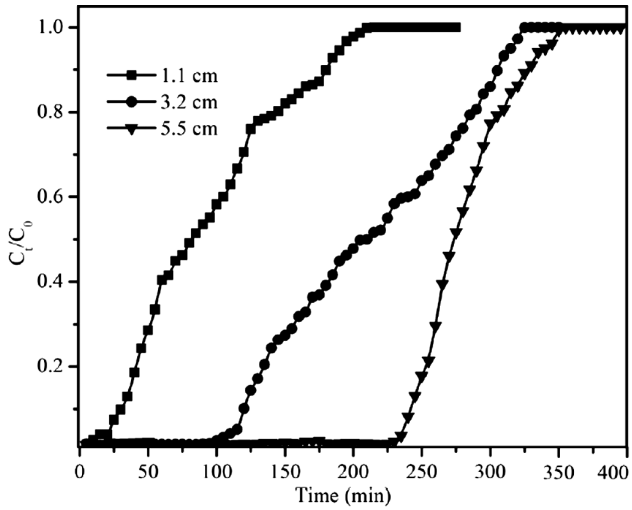

Fig. 3 — Breakthrough curves for packed bed adsorption of AO7 using BFA for different bed height (C_0: 200 mg/L, Q: 2 mL/min)

The effect of influent concentration (100, 200, and 300 mg/L) on the adsorption of AO7 onto BFA is indicated in Fig. 4. The BT curves in Fig. 4 shows that the column is exhausted early for the higher concentration of influent because of limited adsorption sites. This results in the reduction of t_b and t_s values (Table 3), forming the steeper BT curve at greater concentration. The volume of solution treated at breakthrough and saturation is reduced with enhancement in influent concentration. Additionally, the coverage of the BFA surface at higher concentration augments the activation energy which results in the additional adsorption impossible [31]. But the adsorption capacity is found to be enhanced with growth in influent concentration. In Table 3, the capacity of AO7 adsorption for the highest concentration is almost 1.2 times that of the lowest concentration at a constant flow rate and bed height. This increase in capacity is associated with the greater driving force of mass transfer at a higher concentration as compared to that of a lower concentration[31].

Table 3 — Packed bed parameters for removal of AO7 onto BFA

Expt. no	Experimental conditions			Packed bed parameters								
	Bed height (cm)	Influent concentration (mg/L)	Flow rate (mL/min)	V_b (mL)	V_e (mL)	t_b (min)	t_e (min)	t_δ (min)	Adsorption capacity at $t_{0.5}$ (mg/g)	H_{MTZ} (cm)	U_z (cm/min)	% Removal
1	1.1	200	2	17.5	95.0	35	190	38.75	34.00	0.897	0.023	40.25%
2	3.2	200	2	65.0	152.5	130	305	43.75	23.00	1.836	0.042	61.92%
3	5.5	200	2	112.5	177.5	225	355	32.50	22.00	2.014	0.061	76.12%
4	3.2	100	2	132.5	185.0	265	370	26.25	19.67	0.908	0.035	77.66%
5	3.2	200	2	65.0	152.5	130	305	43.75	23.00	1.836	0.042	61.92%
6	3.2	300	2	25.0	95.0	50	190	35.00	26.00	2.358	0.067	30.46%
7	3.2	200	2	65.0	152.5	130	305	43.75	23.00	1.836	0.042	61.92%
8	3.2	200	4	37.5	107.5	75	215	17.50	36.00	2.083	0.120	49.52%
9	3.2	200	6	27. 5	72.5	50	155	8.75	38.00	2.178	0.248	45.84%

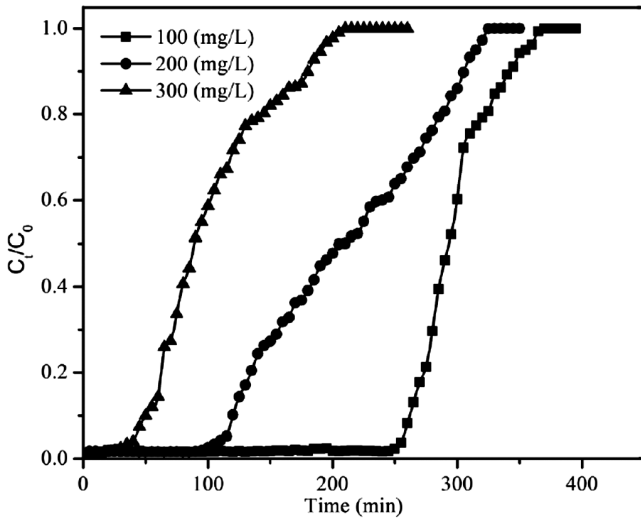

Fig. 4 — Breakthrough curves for packed bed adsorption of AO 7 using BFA for different influent concentration (Z: 3.2 cm ; Q: 2 mL/min)

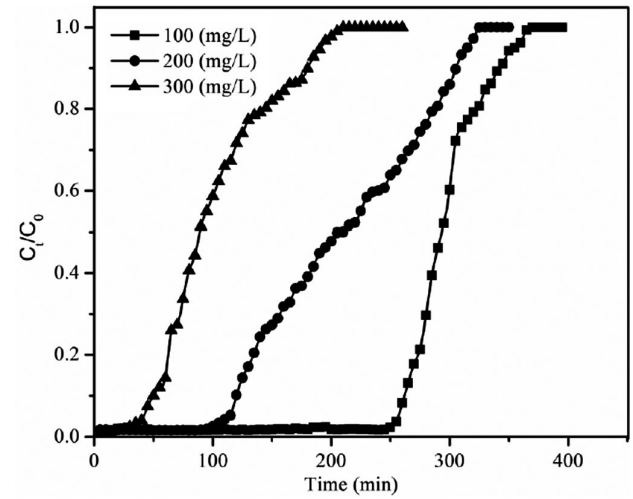

Fig. 5 — Breakthrough curves for packed adsorption of AO 7 using BFA for different flow rate (C_0: 200 mg/L ; Z : 3.2 cm)

The experiments were performed for different flow rates (2, 4, and 6 mL/min) at a constant influent concentration (200 mg/L) and bed height (3.2 cm). The BT curves obtained are presented in Fig. 5 which shows an extended curve for lower flow rate and a steep curve for higher flow rate. The raise in flow rate results in reduced residence time of AO7 in the bed. Consequently, the values of parameters at breakthrough and saturation (t_b, t_e, V_b, and V_e) are reduced for a higher flow rate as shown in Table 3. The lower flow rate tenders sufficient time for AO7 molecules to penetrate into BFA pores, resulting in progressive BT curves. The length of MTZ is increased (Table 3) due to an increase in mass transfer rate with flow rate. Similar results for the length of MTZ are previously reported for pesticide adsorption by Deokar *et al*. (2015)[32]. The reduction in percentage removal for higher flow rate can be attributed to insufficient contact time between AO7 and BFA adsorbent due to the early discharge of AO7 molecules from the BFA bed before equilibrium is achieved.

Application of packed bed models

The efficiency of the packed column in adsorption of AO7 dye using BFA was examined for different models such as BDST, Thomas, Yoon Nelson, Bohard-Adams, and Wolborska models. The linear forms of these models (Table 2) were applied to the column study and the model parameters (Table 4) were determined from the expression. The Thomas model predicts adsorption-desorption kinetics of Langmuir without axial dispersion. The model follows the kinetics of the second-order reversible reaction. The Thomas model is applied here to experimental data in the range $0.01 < (C_t/C_0) < 0.95$

Table 4 — Thomas, Yoon Nelson and Bohart-Adams model parameters for packed bed adsorption of AO7 using BFA

Expt. no	Experimental conditions			Thomas model parameters			Yoon Nelson model parameters				Bohart-Adams model parameters			Wolborska model parameters		
	Z (cm)	C_0 (mg/L)	Q (mL/min)	k_{TH} [L/(g min)]	q_0 (mg/g)	R^2	k_{YN} (min^{-1})	$t_{1/2}$ (τ) (min)	q_{0YN} (mg/g)	R^2	k_{AB} [L/(g min)]	N_o (mg/L)	R^2	β (min^{-1})	N_o (mg/L)	R^2
1	1.1	200	2	1.10×10^{-4}	47.10	0.952	2.80×10^{-2}	89.25	35.70	0.912	2.30×10^{-4}	35780	0.877	8.23	168.50	0.877
2	3.2	200	2	1.20×10^{-4}	29.06	0.961	2.40×10^{-2}	223.79	29.84	0.951	1.05×10^{-4}	38193	0.885	4.01	179.87	0.885
3	5.5	200	2	2.80×10^{-4}	22.89	0.967	1.30×10^{-2}	380.23	30.42	0.578	0.35×10^{-4}	61927	0.416	2.17	291.64	0.416
4	3.2	100	2	3.70×10^{-4}	20.04	0.889	2.80×10^{-2}	307.25	20.48	0.770	1.20×10^{-4}	35284	0.684	4.23	166.17	0.684
5	3.2	200	2	1.20×10^{-4}	29.06	0.961	2.40×10^{-2}	223.79	29.84	0.881	1.05×10^{-4}	38194	0.885	4.01	179.87	0.885
6	3.2	300	2	1.23×10^{-4}	21.01	0.945	3.90×10^{-2}	109.94	21.99	0.930	0.72×10^{-4}	39832	0.734	2.79	187.58	0.734
7	3.2	200	2	1.20×10^{-4}	29.06	0.951	2.40×10^{-2}	223.79	29.84	0.891	1.05×10^{-4}	38194	0.885	4.01	179.87	0.885
8	3.2	200	4	1.75×10^{-4}	35.89	0.990	3.50×10^{-2}	134.57	35.89	0.890	0.73×10^{-4}	74295	0.859	5.20	349.89	0.859
9	3.2	200	6	2.65×10^{-4}	38.08	0.969	6.10×10^{-2}	90.032	36.01	0.952	1.15×10^{-4}	75021	0.882	8.63	353.30	0.882

and the plots obtained are given in Fig .6. Results given in Table 4 show the improvement in the capacity of Thomas model (q_0) with increasing flow rate whereas decrement in capacity with bed height. The kinetic rate constant (k_{TH}) for the Thomas model is increased with augment in bed height and flow rate. This is a result of an increase in the number of active sites due to an increase in bed height and increase in concentration difference with flow rate[33]. A similar trend for results was obtained for the Thomas model by Sadaf *et al* (2015)[34]. The coefficient of determination (R^2) closure to unity indicates the applicability of the model to experimental results.

Yoon-Nelson model proposes that the rate of reduction in the possibility of adsorption of each molecule of adsorbate is proportional to the possibility of adsorbate adsorption[35]. The Yoon-Nelson model is simpler and does not require detailed data regarding the properties of adsorbent. This model is generally applied to estimate the time required for 50% exhaustion of the column. In the present study, the Yoon-Nelson model is applied in a range of between 1and 95% BT of column (Fig. S3 Supplementary Information). The constants of the Yoon-Nelson model in Table 4 depict the reduction in rate constant (k_{YN}) with augmentation in bed height. The values of k_{YN} are increased with increasing flow rate. The predicted time for 50% exhaustion of column is augmented with the rise in bed heightand is reduced with enhancement in influent concentration and bed height. The greater value of bed height enables a lengthy path for AO7 dye molecules to migrate through the bed, consequently the reduced value of rate constant[31].

Bohart-Adams model hypothesizes that the equilibrium of the adsorption process is not instantaneous and the process is continuous[36], therefore the rate of adsorption is directly proportional to the remaining capacity of the adsorbent toward targeted adsorbate and concentraton of the adsorbate[37]. The Bohart-Adams model is applicable to the initial part of the BT curve. Bohart-Adams model applied in this study is shown in Fig. S4 (Supplementary Information). As increasing in bed depth and initial concentration, values of k_{AB} decreases, and N_o increases.

The BDST model provides the detail about the efficacy of column operating under fixed conditions. This model is based on the surface reaction between adsorbate and adsorbent and is a modified form of the

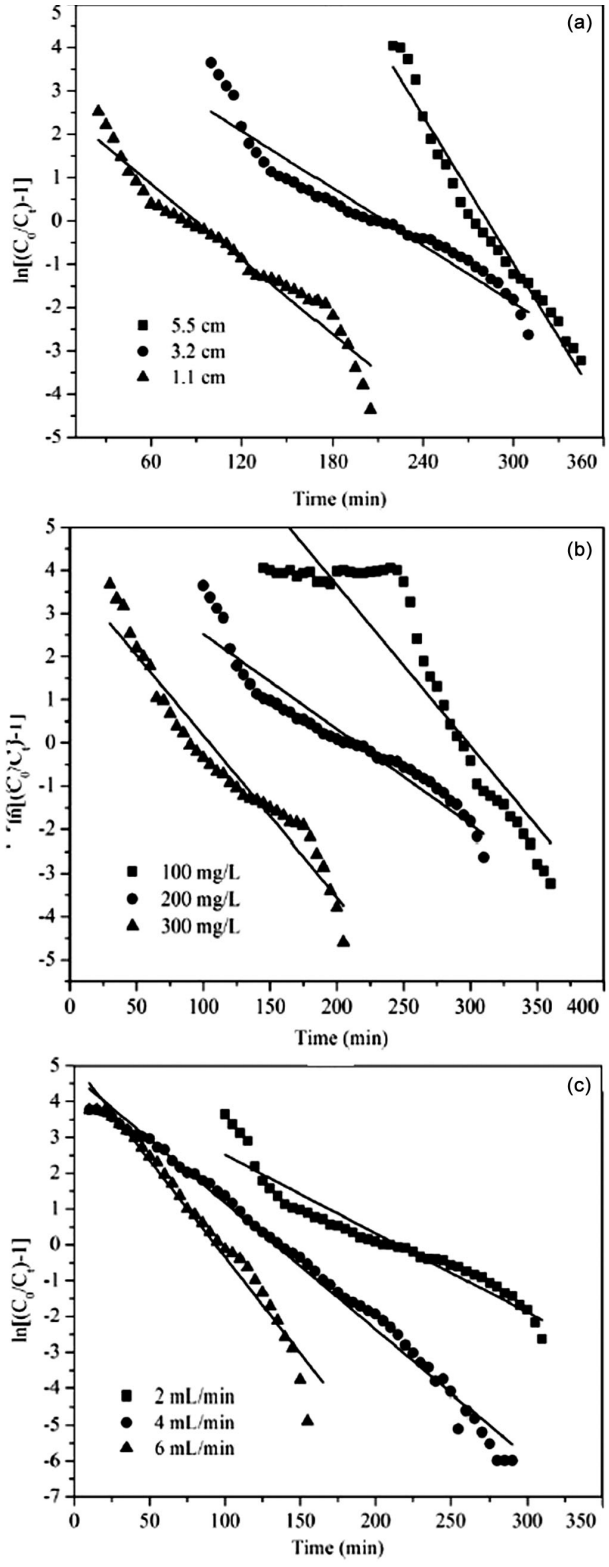

Fig. 6 — Thomas model for packed bed adsorption of AO7 dye using BFA at different (a) bed height (C_0= 200 mg/L; Q= 2 mL/min), (b) influent concentration (Z = 3.2 cm, Q = 2 mL/min) and (c) flow rate (C_0 = 200 mg/L, Z = 3.2 cm)

Bohart-Adams equation. This model is usually applied to measure the capacity of the bed at different BT such as 10%, 50%, and 90% BT of the column. In this study, the bed capacity calculated using the BDST model is found to be24352, 21330, and 16698 (mg/L) at 10%, 50%, and 90% BT of a column at the constant influent concentration (200 mg/L) and flow rate (2 mL/min) respectively. The rate constants ofthe BDST model for 10% and 90% BT are found to be 4.2×10^{-4} and 6.74×10^{-5} [L/(mg min)] respectively. According to the BDST model, adsorption of AO7 on BFA surface is governed by complex mechanisms involving more than one rate-controlling step, which can be seen in Fig. 7, where the 50% breakthrough line (Fig. 7) did not pass through the origin.

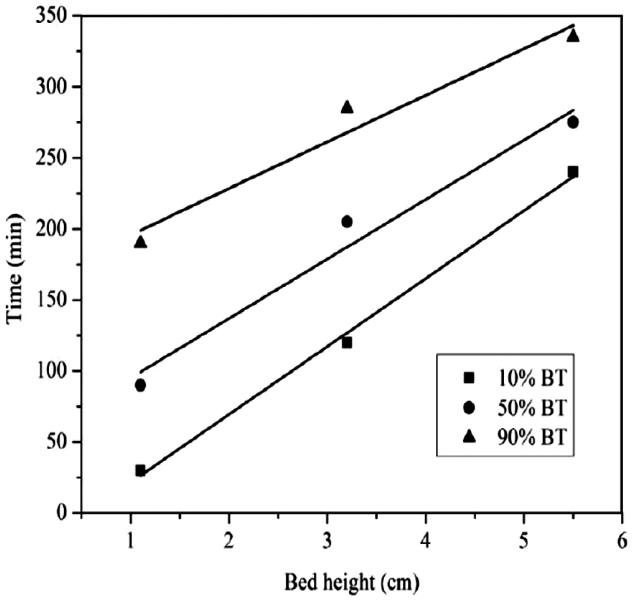

Fig. 7 — Bed depth service time model for packed bed adsorption of AO7 dye using BFA at different bed height (C_0=200 mg/L and Q = 2 mL/min)

Wolborsk a model is generally applied in the region of lower concentration region of the BT curve. The values of parameters of the Wolborska model are presented in Table 4. The rate of mass transfer for the diffusion mechanism is the basis for this model. The mathematical equation of the Wolborska model is comparable to the Bohart-Adams model and therefore the plots of the Wolborska model and Bohart-Adams model are the same (Fig. S4 Supplementary Information). As bed height of BFA column and influent concentration of AO7 dye are increased, Wolborska parameter, β is decreased and adsorption capacity is increased. The comparison of coefficient of determination (R^2) for all the models considered here indicates that R^2 for the Thomas model is higher than that of other models. This conforms to the best fitting of the Thomas model for the packed bed adsorptive removal of AO7 dye onto BFA.

Adsorption capacity of BFA vs other adsorbents

The adsorption capacity of BFA is compared with other adsorbents in Table 5. In most of the adsorption studies using BFA, the batch adsorption capacity of BFA has been determined in previously reported literature. In the present study, the efficacy of BFA as an adsorbent is examined in a packed column, and bed capacity is determined. The comparison of the adsorption capacity of various adsorbents in Table 5 indicates that BFA can be used as an efficient adsorbent for the removal of AO7 dye from an aqueous solution.

Table 5 — Adsorption capacity of BFA vs other adsorbents

Adsorbate	Adsorbent	Type of adsorption	Capacity (mg/g)	Reference
BFA	turquoise blue	Batch	12.66	[38]
BFA	brilliant magenta	Batch	45.45	[38]
BFA	Phenol	Column	9.93	[39]
BFA	Congo red	Batch	11.88	[40]
BFA	Orange-G	Batch	18.79	[41]
BFA	Methyl Violet	Batch	26.24	[41]
BFA	malachite green	Batch	170.33	[42]
Spent brewery grains	acid orange 7	Column	30.50	[43]
Spent brewery grains	acid orange 7	response surface methodology	29.00	[44]
Zero-valent Fe nanoparticles	acid orange 7	Batch	66.6	[45]
macrocomposite	acid orange 7	Batch	0.19	[46]
modified of pumice	acid orange 7	Batch	1.08	[47]
BFA	acid orange 7	Column	38.00	This Study

Conclusions

The characterization of BFA indicates the presence of carbon and silica together with trace quantities of metal oxides. The higher carbon content in BFA plays important role in adsorption of AO7 dye. The packed bed adsorption of AO7 dye using BFA reveals that the adsorption capacity at 50% saturation of column is highest for 3.2 (cm) bed height, 200 (mg /L) concentration and 6 (mL/min) flow rate. For this condition, the treatment of 73 (mL) of solution is carried out. The applicability of different packed bed models to experimental results suggests the best fitting of the Thomas model for the experimental data between 0.1 and 0.95. The adsorption capacity predicted by Thomas model enhances with increasing flow rate indicates the efficient utilization of bed at higher flow rate.

Acknowledgement

The authors are thankful to IBM, Nagpur, and CSMCRI, Bhavnagar (India) for providing sophisticated characterization facilities. The authors thank BARC, Mumbai, for the assistance in characterization studies.

Reference

1 Pathak P D, Mandavgane S A & Kulkarni B D, *Rev Chem Eng*, 31 (2015) 361.
2 Gedam V V, Raut P, Chahande A & Pathak P, *J Appl Water Sci*, 9 (2019) 55.
3 Ojedokun A T & Bell O S, *Appl Water Sci*, 7 (2017) 1965.
4 Ghaedi M, Soylak M, Purkait M K, Hossainian H, Montazerozohori M, Shokrollahi A & Shojaipour F, *Desalination*, 281 (2011) 226.
5 Pathak P D, Singh P & Mandavgane S A, *Indian J Chem Technol*, 25 (2018) 324.
6 Charola S, Das P & Maiti S, *Indian J Chem Technol*, 26 (2019) 35.
7 Charola S, Patel H, Chandna S & Maiti S, *J Clean Prod*, 223 (2019) 969.
8 Srivastava V C, Swamy M M, Mall I D, Prasad B & Mishra I M, *Colloids Surf A: Physicochem Eng, Asp*, 272 (2006) 89.
9 Deokar S K, Mandavgane S A & Kulkarni B D, *Clean Techn Environ Policy*, 18 (2016) 1971.
10 Deokar S K, Mandavgane S A & Kulkarni B D, *Curr Sci*, 110 (2016) 1384.
11 Ahmaruzzaman M, *Prog Energy Combust Sci*, 36 (2010) 327.
12 Dube G, Osifo P & Hilary R, *Clean Technol Environ Policy*, 16 (2014) 891.
13 Patel H, *RSC Adv*, 10 (2020) 31611.
14 Sunil E M & Manavendra G, *Int Res J Eng Technol*, 4 (2017) 444.
15 Kousha M, Daneshvar E, Sohrabi M S, Jokar M & A Bhatnagar, *Chem Eng J*, 192 (2012) 67.
16 Padmesh T V N, Vijayaraghavan K, Sekaran G & Velan M, *Chem Eng J*, 122 (2006) 55.
17 Padmesh T V N, Vijayaraghavan K, Sekaran G & M Velan, *J Hazard Mater*, 125 (2005) 121.
18 Forgacs E, Cserhati T & Oros G, *Environ Int*, 30 (2004) 953.
19 Zee F P V D & Villaverde S, *Water Res*, 39 (2005) 1425.
20 Peng Y, Fu D, Liu R, Zhang F & Liang X, *Chemosphere*, 71 (2008) 990.
21 Aber S, Daneshvar N, Soroureddin S M, Chabok A & Asadpour-Zeynali K, *Desalination*, 211 (2007) 87.
22 I. 1350, (Indian Standard "Methods of test for coal and coke PART I : proximate analysis (Second Revision) IS : 1350" July (2006).
23 Unuabonah E I, Olu-Owolabi B I, Fasuyi E I & Adebowale K O, *J Hazard Mater*, 179 (2010) 415.
24 Chowdhury Z Z, Hamid S B A & Zain S M, *Bio Resour*, 10 (2015) 732.
25 Srivastava V C, Prasad B, Mishra I M, Mall I D & Swamy M M, *Indust Eng Chem Res*, 47 (2008) 1603.
26 Chatterjee A & Schiewer S, *Chem Eng J*, 244 (2014) 105.
27 Xavier A LP, Adarme O F H, Furtado L M, Ferreira G M D, da Silva L H M, Gil L F & Gurgel L V A, *J Colloid Interf Sci*, 516 (2018) 431.
28 Charola S, Yadav R, Das P & Maiti S, *Sust Environ Res*, 28 (2018) 298.
29 Brunauer S, Emmett P H & Teller E, *J Am Chem Soc*, 60 (1938) 309.
30 Stylidi M, Kondarides D I & Verykios X E, *Appl Catal B: Environ*, 47 (2004) 189.
31 Deokar S K, Mandavgane S A & Kulkarni B D, *J Environ Chem Eng*, 3 (2015) 1827.
32 Deokar S K & Mandavgane S A, *J Environ Chem Eng*, 3 (2015) 1827.
33 Deokar S K, Mandavgane S A & Kulkarni B D, *Desalination Water Treat*, 57 (2016) 28831.
34 Sadaf S, Bhatti H N, Nausheen S & Amin M, *J Taiwan Inst Chem Eng*, 47 (2015) 160.
35 Salman J M, Njokua V O & Hameed B H, *Chem Eng J*, 174 (2011) 33.
36 Nawaz S, Bhatti H N, Bokhari T H & Sadaf S, *Chem Ecol*, 30 (2014) 52.
37 Sadaf S & Bhatti H N, *J Taiwan Inst Chem Eng*, 45 (2014) 541.
38 Shah B A, Shah A V, Patel H D & Mistry C B, *Water Environ Res*, 85 (2013) 558.
39 Srivastava V C, Prasad B, Mishra I M, Mall I D & Swamy M M, *Ind Eng Chem Res*, 47 (2008) 1603.
40 Mall I D, Srivastava V C, Agarwal N K & Mishra I M, *Chemosphere*, 61 (2005) 492.
41 Mall I D, Srivastava V C & Agarwal N K, *Dyes Pigm*, 69 (2006) 210.
42 Mall I D, Srivastava V C, Agarwal N K & Mishra I M, *Colloids Surf A: Physicochem Eng Asp*, 264 (2005) 17.
43 Pedro Silva J, Sousa S, Rodrigues J, Antunes H, Porter J J, Gonçalves I & Ferreira-Dias S, *Sep Purif Technol*, 40 (2004) 309.
44 Silva J P, Sousa S, Gonçalves I, Porter J J & Ferreira-Dias S, *Sep Purif Technol*, 40 (2004) 163.
45 Zaheer Z, AbuBaker Bawazir W, Al-Bukhari S M & Basaleh A S, Mater Chem Phys, 232 (2019) 109.
46 Lim C K, Bay H H, Neoh C H, Aris A, Abdul Majid Z & Ibrahim Z, *Environ Sci Pollut Res Int*, 20 (2013) 7243.
47 Ahmadian M, Yosefi N, Toolabi A, Khanjani N, Rahimi-Keshari S & Fatehizadeh A, *Asian J Chem*, 24 (2012) 3094.